

8-31-2011

Observation of the Ξ_b^0 baryon

T. Aaltonen
Helsingin Yliopisto

B. Álvarez González
Universidad de Cantabria

S. Amerio
Istituto Nazionale Di Fisica Nucleare, Sezione di Padova

D. Amidei
University of Michigan, Ann Arbor

A. Anastassov
Northwestern University

See next page for additional authors

Follow this and additional works at: https://digitalcommons.lsu.edu/physics_astronomy_pubs

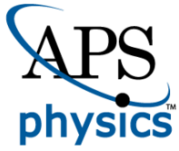
Recommended Citation

Aaltonen, T., Álvarez González, B., Amerio, S., Amidei, D., Anastassov, A., Annovi, A., Antos, J., Apollinari, G., Appel, J., Apresyan, A., Arisawa, T., Artikov, A., Asaadi, J., Ashmanskas, W., Auerbach, B., Aurisano, A., Azfar, F., Badgett, W., Barbaro-Galtieri, A., Barnes, V., Barnett, B., Barria, P., Bartos, P., Bauce, M., Bauer, G., Bedeschi, F., Beecher, D., & Behari, S. (2011). Observation of the Ξ_b^0 baryon. *Physical Review Letters*, 107(10) <https://doi.org/10.1103/PhysRevLett.107.102001>

This Article is brought to you for free and open access by the Department of Physics & Astronomy at LSU Digital Commons. It has been accepted for inclusion in Faculty Publications by an authorized administrator of LSU Digital Commons. For more information, please contact ir@lsu.edu.

Authors

T. Aaltonen, B. Álvarez González, S. Amerio, D. Amidei, A. Anastassov, A. Annovi, J. Antos, G. Apollinari, J. A. Appel, A. Apresyan, T. Arisawa, A. Artikov, J. Asaadi, W. Ashmanskas, B. Auerbach, A. Aurisano, F. Azfar, W. Badgett, A. Barbaro-Galtieri, V. E. Barnes, B. A. Barnett, P. Barria, P. Bartos, M. Bauce, G. Bauer, F. Bedeschi, D. Beecher, and S. Behari



CHORUS

This is the accepted manuscript made available via CHORUS. The article has been published as:

Observation of the $\Xi_{\text{b}}^{\{0\}}$ Baryon

T. Aaltonen *et al.* (CDF Collaboration)

Phys. Rev. Lett. **107**, 102001 — Published 31 August 2011

DOI: [10.1103/PhysRevLett.107.102001](https://doi.org/10.1103/PhysRevLett.107.102001)

Observation of the Ξ_b^0 Baryon

T. Aaltonen,²¹ B. Álvarez González^{w,9} S. Amerio,⁴¹ D. Amidei,³² A. Anastassov,³⁶ A. Annovi,¹⁷ J. Antos,¹²
 G. Apollinari,¹⁵ J.A. Appel,¹⁵ A. Apresyan,⁴⁶ T. Arisawa,⁵⁶ A. Artikov,¹³ J. Asaadi,⁵¹ W. Ashmanskas,¹⁵
 B. Auerbach,⁵⁹ A. Aurisano,⁵¹ F. Azfar,⁴⁰ W. Badgett,¹⁵ A. Barbaro-Galtieri,²⁶ V.E. Barnes,⁴⁶ B.A. Barnett,²³
 P. Barria^{dd,44} P. Bartos,¹² M. Bauce^{bb,41} G. Bauer,³⁰ F. Bedeschi,⁴⁴ D. Beecher,²⁸ S. Behari,²³ G. Bellettini^{cc,44}
 J. Bellinger,⁵⁸ D. Benjamin,¹⁴ A. Beretvas,¹⁵ A. Bhatti,⁴⁸ M. Binkley^{*,15} D. Bisello^{bb,41} I. Bizjak^{hh,28} K.R. Bland,⁵
 B. Blumenfeld,²³ A. Bocci,¹⁴ A. Bodek,⁴⁷ D. Bortoletto,⁴⁶ J. Boudreau,⁴⁵ A. Boveia,¹¹ L. Brigliadori^{aa,6}
 A. Brisuda,¹² C. Bromberg,³³ E. Brucken,²¹ M. Bucciantonio^{cc,44} J. Budagov,¹³ H.S. Budd,⁴⁷ S. Budd,²²
 K. Burkett,¹⁵ G. Busetto^{bb,41} P. Bussey,¹⁹ A. Buzatu,³¹ C. Calancha,²⁹ S. Camarda,⁴ M. Campanelli,²⁸
 M. Campbell,³² F. Canelli^{11,15} B. Carls,²² D. Carlsmith,⁵⁸ R. Carosi,⁴⁴ S. Carrillo^{k,16} S. Carron,¹⁵ B. Casal,⁹
 M. Casarsa,¹⁵ A. Castro^{aa,6} P. Catastini,²⁰ D. Cauz,⁵² V. Cavaliere,²² M. Cavalli-Sforza,⁴ A. Cerri^{e,26}
 L. Cerrito^{q,28} Y.C. Chen,¹ M. Chertok,⁷ G. Chiarelli,⁴⁴ G. Chlachidze,¹⁵ F. Chlebana,¹⁵ K. Cho,²⁵
 D. Chokheli,¹³ J.P. Chou,²⁰ W.H. Chung,⁵⁸ Y.S. Chung,⁴⁷ C.I. Ciobanu,⁴² M.A. Ciocci^{dd,44} A. Clark,¹⁸
 C. Clarke,⁵⁷ G. Compostella^{bb,41} M.E. Convery,¹⁵ J. Conway,⁷ M. Corbo,⁴² M. Cordelli,¹⁷ C.A. Cox,⁷ D.J. Cox,⁷
 F. Crescioli^{cc,44} C. Cuenca Almenar,⁵⁹ J. Cuevas^{w,9} R. Culbertson,¹⁵ D. Dagenhart,¹⁵ N. d'Ascenzo^{u,42}
 M. Datta,¹⁵ P. de Barbaro,⁴⁷ S. De Cecco,⁴⁹ G. De Lorenzo,⁴ M. Dell'Orso^{cc,44} C. Deluca,⁴ L. Demortier,⁴⁸
 J. Deng^{b,14} M. Deninno,⁶ F. Devoto,²¹ M. d'Errico^{bb,41} A. Di Canto^{cc,44} B. Di Ruzza,⁴⁴ J.R. Dittmann,⁵
 M. D'Onofrio,²⁷ S. Donati^{cc,44} P. Dong,¹⁵ M. Dorigo,⁵² T. Dorigo,⁴¹ K. Ebina,⁵⁶ A. Elagin,⁵¹ A. Eppig,³²
 R. Erbacher,⁷ D. Errede,²² S. Errede,²² N. Ershaidat^{z,42} R. Eusebi,⁵¹ H.C. Fang,²⁶ S. Farrington,⁴⁰ M. Feindt,²⁴
 J.P. Fernandez,²⁹ C. Ferrazza^{ee,44} R. Field,¹⁶ G. Flanagan^{s,46} R. Forrest,⁷ M.J. Frank,⁵ M. Franklin,²⁰
 J.C. Freeman,¹⁵ Y. Funakoshi,⁵⁶ I. Furic,¹⁶ M. Gallinaro,⁴⁸ J. Galyardt,¹⁰ J.E. Garcia,¹⁸ A.F. Garfinkel,⁴⁶
 P. Garosi^{dd,44} H. Gerberich,²² E. Gerchtein,¹⁵ S. Giagu^{ff,49} V. Giakoumopoulou,³ P. Giannetti,⁴⁴ K. Gibson,⁴⁵
 C.M. Ginsburg,¹⁵ N. Giokaris,³ P. Giromini,¹⁷ M. Giunta,⁴⁴ G. Giurgiu,²³ V. Glagolev,¹³ D. Glenzinski,¹⁵
 M. Gold,³⁵ D. Goldin,⁵¹ N. Goldschmidt,¹⁶ A. Golossanov,¹⁵ G. Gomez,⁹ G. Gomez-Ceballos,³⁰ M. Goncharov,³⁰
 O. González,²⁹ I. Gorelov,³⁵ A.T. Goshaw,¹⁴ K. Goulianos,⁴⁸ S. Grinstein,⁴ C. Grosso-Pilcher,¹¹ R.C. Group^{55,15}
 J. Guimaraes da Costa,²⁰ Z. Gunay-Unalan,³³ C. Haber,²⁶ S.R. Hahn,¹⁵ E. Halkiadakis,⁵⁰ A. Hamaguchi,³⁹
 J.Y. Han,⁴⁷ F. Happacher,¹⁷ K. Hara,⁵³ D. Hare,⁵⁰ M. Hare,⁵⁴ R.F. Harr,⁵⁷ K. Hatakeyama,⁵ C. Hays,⁴⁰ M. Heck,²⁴
 J. Heinrich,⁴³ M. Herndon,⁵⁸ S. Hewamanage,⁵ D. Hidas,⁵⁰ A. Hocker,¹⁵ W. Hopkins^{f,15} D. Horn,²⁴ S. Hou,¹
 R.E. Hughes,³⁷ M. Hurwitz,¹¹ U. Husemann,⁵⁹ N. Hussain,³¹ M. Hussein,³³ J. Huston,³³ G. Introzzi,⁴⁴ M. Iori^{ff,49}
 A. Ivanov^{o,7} E. James,¹⁵ D. Jang,¹⁰ B. Jayatilaka,¹⁴ E.J. Jeon,²⁵ M.K. Jha,⁶ S. Jindariani,¹⁵ W. Johnson,⁷
 M. Jones,⁴⁶ K.K. Joo,²⁵ S.Y. Jun,¹⁰ T.R. Junk,¹⁵ T. Kamon,⁵¹ P.E. Karchin,⁵⁷ A. Kasmi,⁵ Y. Kato^{n,39}
 W. Ketchum,¹¹ J. Keung,⁴³ V. Khotilovich,⁵¹ B. Kilminster,¹⁵ D.H. Kim,²⁵ H.S. Kim,²⁵ H.W. Kim,²⁵ J.E. Kim,²⁵
 M.J. Kim,¹⁷ S.B. Kim,²⁵ S.H. Kim,⁵³ Y.K. Kim,¹¹ N. Kimura,⁵⁶ M. Kirby,¹⁵ S. Klimentenko,¹⁶ K. Kondo^{*,56}
 D.J. Kong,²⁵ J. Konigsberg,¹⁶ A.V. Kotwal,¹⁴ M. Kreps,²⁴ J. Kroll,⁴³ D. Krop,¹¹ N. Krumnack^{l,5} M. Kruse,¹⁴
 V. Krutelyov^{c,51} T. Kuhr,²⁴ M. Kurata,⁵³ S. Kwang,¹¹ A.T. Laasanen,⁴⁶ S. Lami,⁴⁴ S. Lammel,¹⁵ M. Lancaster,²⁸
 R.L. Lander,⁷ K. Lannon^{v,37} A. Lath,⁵⁰ G. Latino^{cc,44} T. LeCompte,² E. Lee,⁵¹ H.S. Lee,¹¹ J.S. Lee,²⁵ S.W. Lee^{x,51}
 S. Leo^{cc,44} S. Leone,⁴⁴ J.D. Lewis,¹⁵ A. Limosani^{r,14} C.-J. Lin,²⁶ J. Linacre,⁴⁰ M. Lindgren,¹⁵ E. Lipeles,⁴³
 A. Lister,¹⁸ D.O. Litvintsev,¹⁵ C. Liu,⁴⁵ Q. Liu,⁴⁶ T. Liu,¹⁵ S. Lockwitz,⁵⁹ A. Loginov,⁵⁹ D. Lucchesi^{bb,41}
 J. Lueck,²⁴ P. Lujan,²⁶ P. Lukens,¹⁵ G. Lungu,⁴⁸ J. Lys,²⁶ R. Lysak,¹² R. Madrak,¹⁵ K. Maeshima,¹⁵
 K. Makhoul,³⁰ S. Malik,⁴⁸ G. Manca^{a,27} A. Manousakis-Katsikakis,³ F. Margaroli,⁴⁶ C. Marino,²⁴ M. Martínez,⁴
 R. Martínez-Ballarín,²⁹ P. Mastrandrea,⁴⁹ M.E. Mattson,⁵⁷ P. Mazzanti,⁶ K.S. McFarland,⁴⁷ P. McIntyre,⁵¹
 R. McNulty^{i,27} A. Mehta,²⁷ P. Mehtala,²¹ A. Menzione,⁴⁴ C. Mesropian,⁴⁸ T. Miao,¹⁵ D. Mietlicki,³² A. Mitra,¹
 H. Miyake,⁵³ S. Moed,²⁰ N. Moggi,⁶ M.N. Mondragon^{k,15} C.S. Moon,²⁵ R. Moore,¹⁵ M.J. Morello,¹⁵ J. Morlock,²⁴
 P. Movilla Fernandez,¹⁵ A. Mukherjee,¹⁵ Th. Muller,²⁴ P. Murat,¹⁵ M. Mussini^{aa,6} J. Nachtman^{m,15} Y. Nagai,⁵³
 J. Naganoma,⁵⁶ I. Nakano,³⁸ A. Napier,⁵⁴ J. Nett,⁵¹ C. Neu,⁵⁵ M.S. Neubauer,²² J. Nielsen^{d,26} L. Nodulman,²
 O. Norriella,²² E. Nurse,²⁸ L. Oakes,⁴⁰ S.H. Oh,¹⁴ Y.D. Oh,²⁵ I. Oksuzian,⁵⁵ T. Okusawa,³⁹ R. Orava,²¹
 L. Ortolan,⁴ S. Pagan Griso^{bb,41} C. Pagliarone,⁵² E. Palencia^{e,9} V. Papadimitriou,¹⁵ A.A. Paramonov,²
 J. Patrick,¹⁵ G. Pauletta^{gg,52} M. Paulini,¹⁰ C. Paus,³⁰ D.E. Pellett,⁷ A. Penzo,⁵² T.J. Phillips,¹⁴ G. Piacentino,⁴⁴
 E. Pianori,⁴³ J. Pilot,³⁷ K. Pitts,²² C. Plager,⁸ L. Pondrom,⁵⁸ K. Potamianos,⁴⁶ O. Poukhov^{*,13} F. Prokoshin^{y,13}
 A. Pronko,¹⁵ F. Ptohos^{g,17} E. Pueschel,¹⁰ G. Punzi^{cc,44} J. Pursley,⁵⁸ A. Rahaman,⁴⁵ V. Ramakrishnan,⁵⁸
 N. Ranjan,⁴⁶ I. Redondo,²⁹ P. Renton,⁴⁰ M. Rescigno,⁴⁹ T. Riddick,²⁸ F. Rimondi^{aa,6} L. Ristori^{44,15} A. Robson,¹⁹

T. Rodrigo,⁹ T. Rodriguez,⁴³ E. Rogers,²² S. Rolli^h,⁵⁴ R. Roser,¹⁵ M. Rossi,⁵² F. Rubbo,¹⁵ F. Ruffini^{dd},⁴⁴
 A. Ruiz,⁹ J. Russ,¹⁰ V. Rusu,¹⁵ A. Safonov,⁵¹ W.K. Sakumoto,⁴⁷ Y. Sakurai,⁵⁶ L. Santi^{gg},⁵² L. Sartori,⁴⁴
 K. Sato,⁵³ V. Saveliev^u,⁴² A. Savoy-Navarro,⁴² P. Schlabach,¹⁵ A. Schmidt,²⁴ E.E. Schmidt,¹⁵ M.P. Schmidt^{*},⁵⁹
 M. Schmitt,³⁶ T. Schwarz,⁷ L. Scodellaro,⁹ A. Scribano^{dd},⁴⁴ F. Scuri,⁴⁴ A. Sedov,⁴⁶ S. Seidel,³⁵ Y. Seiya,³⁹
 A. Semenov,¹³ F. Sforza^{cc},⁴⁴ A. Sfyrta,²² S.Z. Shalhout,⁷ T. Shears,²⁷ P.F. Shepard,⁴⁵ M. Shimojima^t,⁵³
 S. Shiraishi,¹¹ M. Shochet,¹¹ I. Shreyber,³⁴ A. Simonenko,¹³ P. Sinervo,³¹ A. Sissakian^{*},¹³ K. Sliwa,⁵⁴ J.R. Smith,⁷
 F.D. Snider,¹⁵ A. Soha,¹⁵ S. Somalwar,⁵⁰ V. Sorin,⁴ P. Squillacioti,⁴⁴ M. Stancari,¹⁵ M. Stanitzki,⁵⁹
 R. St. Denis,¹⁹ B. Stelzer,³¹ O. Stelzer-Chilton,³¹ D. Stentz,³⁶ J. Strologas,³⁵ G.L. Strycker,³² Y. Sudo,⁵³
 A. Sukhanov,¹⁶ I. Suslov,¹³ K. Takemasa,⁵³ Y. Takeuchi,⁵³ J. Tang,¹¹ M. Tecchio,³² P.K. Teng,¹ J. Thom^f,¹⁵
 J. Thome,¹⁰ G.A. Thompson,²² E. Thomson,⁴³ P. Ttito-Guzmán,²⁹ S. Tkaczyk,¹⁵ D. Toback,⁵¹ S. Tokar,¹²
 K. Tollefson,³³ T. Tomura,⁵³ D. Tonelli,¹⁵ S. Torre,¹⁷ D. Torretta,¹⁵ P. Totaro,⁴¹ M. Trovato^{ee},⁴⁴ Y. Tu,⁴³
 F. Ukegawa,⁵³ S. Uozumi,²⁵ A. Varganov,³² F. Vázquez^k,¹⁶ G. Velez,¹⁵ C. Vellidis,³ M. Vidal,²⁹ I. Vila,⁹
 R. Vilar,⁹ J. Vizán,⁹ M. Vogel,³⁵ G. Volpi^{cc},⁴⁴ P. Wagner,⁴³ R.L. Wagner,¹⁵ T. Wakisaka,³⁹ R. Wallny,⁸
 S.M. Wang,¹ A. Warburton,³¹ D. Waters,²⁸ M. Weinberger,⁵¹ W.C. Wester III,¹⁵ B. Whitehouse,⁵⁴ D. Whiteson^b,⁴³
 A.B. Wicklund,² E. Wicklund,¹⁵ S. Wilbur,¹¹ F. Wick,²⁴ H.H. Williams,⁴³ J.S. Wilson,³⁷ P. Wilson,¹⁵ B.L. Winer,³⁷
 P. Wittich^g,¹⁵ S. Wolbers,¹⁵ H. Wolfe,³⁷ T. Wright,³² X. Wu,¹⁸ Z. Wu,⁵ K. Yamamoto,³⁹ J. Yamaoka,¹⁴
 T. Yang,¹⁵ U.K. Yang^p,¹¹ Y.C. Yang,²⁵ W.-M. Yao,²⁶ G.P. Yeh,¹⁵ K. Yi^m,¹⁵ J. Yoh,¹⁵ K. Yorita,⁵⁶
 T. Yoshida^j,³⁹ G.B. Yu,¹⁴ I. Yu,²⁵ S.S. Yu,¹⁵ J.C. Yun,¹⁵ A. Zanetti,⁵² Y. Zeng,¹⁴ and S. Zucchelli^{aa6}

(CDF Collaboration[†])

¹*Institute of Physics, Academia Sinica, Taipei, Taiwan 11529, Republic of China*

²*Argonne National Laboratory, Argonne, Illinois 60439, USA*

³*University of Athens, 157 71 Athens, Greece*

⁴*Institut de Física d'Altes Energies, ICREA, Universitat Autònoma de Barcelona, E-08193, Bellaterra (Barcelona), Spain*

⁵*Baylor University, Waco, Texas 76798, USA*

⁶*Istituto Nazionale di Fisica Nucleare Bologna, ^{aa}University of Bologna, I-40127 Bologna, Italy*

⁷*University of California, Davis, Davis, California 95616, USA*

⁸*University of California, Los Angeles, Los Angeles, California 90024, USA*

⁹*Instituto de Física de Cantabria, CSIC-University of Cantabria, 39005 Santander, Spain*

¹⁰*Carnegie Mellon University, Pittsburgh, Pennsylvania 15213, USA*

¹¹*Enrico Fermi Institute, University of Chicago, Chicago, Illinois 60637, USA*

¹²*Comenius University, 842 48 Bratislava, Slovakia; Institute of Experimental Physics, 040 01 Kosice, Slovakia*

¹³*Joint Institute for Nuclear Research, RU-141980 Dubna, Russia*

¹⁴*Duke University, Durham, North Carolina 27708, USA*

¹⁵*Fermi National Accelerator Laboratory, Batavia, Illinois 60510, USA*

¹⁶*University of Florida, Gainesville, Florida 32611, USA*

¹⁷*Laboratori Nazionali di Frascati, Istituto Nazionale di Fisica Nucleare, I-00044 Frascati, Italy*

¹⁸*University of Geneva, CH-1211 Geneva 4, Switzerland*

¹⁹*Glasgow University, Glasgow G12 8QQ, United Kingdom*

²⁰*Harvard University, Cambridge, Massachusetts 02138, USA*

²¹*Division of High Energy Physics, Department of Physics,
University of Helsinki and Helsinki Institute of Physics, FIN-00014, Helsinki, Finland*

²²*University of Illinois, Urbana, Illinois 61801, USA*

²³*The Johns Hopkins University, Baltimore, Maryland 21218, USA*

²⁴*Institut für Experimentelle Kernphysik, Karlsruhe Institute of Technology, D-76131 Karlsruhe, Germany*

²⁵*Center for High Energy Physics: Kyungpook National University,*

Daegu 702-701, Korea; Seoul National University, Seoul 151-742,

Korea; Sungkyunkwan University, Suwon 440-746,

Korea; Korea Institute of Science and Technology Information,

Daejeon 305-806, Korea; Chonnam National University, Gwangju 500-757,

Korea; Chonbuk National University, Jeonju 561-756, Korea

²⁶*Ernest Orlando Lawrence Berkeley National Laboratory, Berkeley, California 94720, USA*

²⁷*University of Liverpool, Liverpool L69 7ZE, United Kingdom*

²⁸*University College London, London WC1E 6BT, United Kingdom*

²⁹*Centro de Investigaciones Energeticas Medioambientales y Tecnológicas, E-28040 Madrid, Spain*

³⁰*Massachusetts Institute of Technology, Cambridge, Massachusetts 02139, USA*

³¹*Institute of Particle Physics: McGill University, Montréal, Québec,
Canada H3A 2T8; Simon Fraser University, Burnaby, British Columbia,*

Canada V5A 1S6; University of Toronto, Toronto, Ontario,

Canada M5S 1A7; and TRIUMF, Vancouver, British Columbia, Canada V6T 2A3

- ³²University of Michigan, Ann Arbor, Michigan 48109, USA
³³Michigan State University, East Lansing, Michigan 48824, USA
³⁴Institution for Theoretical and Experimental Physics, ITEP, Moscow 117259, Russia
³⁵University of New Mexico, Albuquerque, New Mexico 87131, USA
³⁶Northwestern University, Evanston, Illinois 60208, USA
³⁷The Ohio State University, Columbus, Ohio 43210, USA
³⁸Okayama University, Okayama 700-8530, Japan
³⁹Osaka City University, Osaka 588, Japan
⁴⁰University of Oxford, Oxford OX1 3RH, United Kingdom
⁴¹Istituto Nazionale di Fisica Nucleare, Sezione di Padova-Trento, ^{bb}University of Padova, I-35131 Padova, Italy
⁴²LPNHE, Universite Pierre et Marie Curie/IN2P3-CNRS, UMR7585, Paris, F-75252 France
⁴³University of Pennsylvania, Philadelphia, Pennsylvania 19104, USA
⁴⁴Istituto Nazionale di Fisica Nucleare Pisa, ^{cc}University of Pisa,
^{dd}University of Siena and ^{ee}Scuola Normale Superiore, I-56127 Pisa, Italy
⁴⁵University of Pittsburgh, Pittsburgh, Pennsylvania 15260, USA
⁴⁶Purdue University, West Lafayette, Indiana 47907, USA
⁴⁷University of Rochester, Rochester, New York 14627, USA
⁴⁸The Rockefeller University, New York, New York 10065, USA
⁴⁹Istituto Nazionale di Fisica Nucleare, Sezione di Roma 1,
^{ff}Sapienza Università di Roma, I-00185 Roma, Italy
⁵⁰Rutgers University, Piscataway, New Jersey 08855, USA
⁵¹Texas A&M University, College Station, Texas 77843, USA
⁵²Istituto Nazionale di Fisica Nucleare Trieste/Udine,
I-34100 Trieste, ^{gg}University of Udine, I-33100 Udine, Italy
⁵³University of Tsukuba, Tsukuba, Ibaraki 305, Japan
⁵⁴Tufts University, Medford, Massachusetts 02155, USA
⁵⁵University of Virginia, Charlottesville, Virginia 22906, USA
⁵⁶Waseda University, Tokyo 169, Japan
⁵⁷Wayne State University, Detroit, Michigan 48201, USA
⁵⁸University of Wisconsin, Madison, Wisconsin 53706, USA
⁵⁹Yale University, New Haven, Connecticut 06520, USA

The observation of the bottom, strange baryon Ξ_b^0 through the decay chain $\Xi_b^0 \rightarrow \Xi_c^+ \pi^-$, where $\Xi_c^+ \rightarrow \Xi^- \pi^+ \pi^+$, $\Xi^- \rightarrow \Lambda \pi^-$, and $\Lambda \rightarrow p \pi^-$, is reported using data corresponding to an integrated luminosity of 4.2 fb^{-1} from $p\bar{p}$ collisions at $\sqrt{s} = 1.96 \text{ TeV}$ recorded with the Collider Detector at Fermilab. A signal of $25.3_{-5.4}^{+5.6}$ candidates is observed whose probability of arising from a background fluctuation is 3.6×10^{-12} , corresponding to 6.8 Gaussian standard deviations. The Ξ_b^0 mass is measured to be $5787.8 \pm 5.0(\text{stat}) \pm 1.3(\text{syst}) \text{ MeV}/c^2$. In addition, the Ξ_b^- baryon is observed through the process $\Xi_b^- \rightarrow \Xi_c^0 \pi^-$, where $\Xi_c^0 \rightarrow \Xi^- \pi^+$, $\Xi^- \rightarrow \Lambda \pi^-$, and $\Lambda \rightarrow p \pi^-$.

PACS numbers: 13.30.Eg, 13.60.Rj, 14.20.Mr

*Deceased

†With visitors from ^aIstituto Nazionale di Fisica Nucleare, Sezione di Cagliari, 09042 Monserrato (Cagliari), Italy, ^bUniversity of CA Irvine, Irvine, CA 92697, USA, ^cUniversity of CA Santa Barbara, Santa Barbara, CA 93106, USA, ^dUniversity of CA Santa Cruz, Santa Cruz, CA 95064, USA, ^eCERN, CH-1211 Geneva, Switzerland, ^fCornell University, Ithaca, NY 14853, USA, ^gUniversity of Cyprus, Nicosia CY-1678, Cyprus, ^hOffice of Science, U.S. Department of Energy, Washington, DC 20585, USA, ⁱUniversity College Dublin, Dublin 4, Ireland, ^jUniversity of Fukui, Fukui City, Fukui Prefecture, Japan 910-0017, ^kUniversidad Iberoamericana, Mexico D.F., Mexico, ^lIowa State University, Ames, IA 50011, USA, ^mUniversity of Iowa, Iowa City, IA 52242, USA, ⁿKinki University, Higashi-Osaka City, Japan 577-8502, ^oKansas State University, Manhattan, KS 66506, USA, ^pUniversity of Manchester, Manchester M13 9PL, United Kingdom, ^qQueen Mary, University of London, London, E1 4NS, United Kingdom, ^rUniversity of Melbourne, Victoria 3010, Australia, ^sMuons, Inc., Batavia, IL 60510, USA, ^tNagasaki Institute of Applied Science, Nagasaki, Japan, ^uNational

The quark model has had great success in describing the spectroscopy of hadrons. For the c and b mesons, all of the ground states have been observed [1]. The spectroscopy of c baryons also agrees well with the quark model, and a rich spectrum of baryons containing b quarks is predicted [2]. Until recently, direct observation of b baryons has been limited to a single state, the Λ_b^0 (quark content $|udb\rangle$) [1]. The accumulation of large data sets from the Tevatron has improved this situation and made possible the observation of the Ξ_b^- ($|dsb\rangle$) [3, 4], the

Research Nuclear University, Moscow, Russia, ^vUniversity of Notre Dame, Notre Dame, IN 46556, USA, ^wUniversidad de Oviedo, E-33007 Oviedo, Spain, ^xTexas Tech University, Lubbock, TX 79609, USA, ^yUniversidad Tecnica Federico Santa Maria, 110v Valparaiso, Chile, ^zYarmouk University, Irbid 211-63, Jordan, ^{hh}On leave from J. Stefan Institute, Ljubljana, Slovenia,

$\Sigma_b^{(*)}$ states ($|uub\rangle, |ddb\rangle$) [5], and the Ω_b ($|ssb\rangle$) [6, 7].

In this paper, we report the observation of an additional heavy baryon and the measurement of its mass. The decay properties of this state are consistent with the weak decay of a b baryon. We interpret the result as the observation of the Ξ_b^0 baryon ($|usb\rangle$). This measurement is made in $p\bar{p}$ collisions at a center of mass energy of 1.96 TeV using the Collider Detector at Fermilab (CDF II), by fully reconstructing the decay chain $\Xi_b^0 \rightarrow \Xi_c^+ \pi^-$, where $\Xi_c^+ \rightarrow \Xi^- \pi^+ \pi^+$, $\Xi^- \rightarrow \Lambda \pi^-$, and $\Lambda \rightarrow p \pi^-$. Charge conjugate modes are included implicitly. In addition, we observe the Ξ_b^- through the similar decay chain $\Xi_b^- \rightarrow \Xi_c^0 \pi^-$, where $\Xi_c^0 \rightarrow \Xi^- \pi^+$, $\Xi^- \rightarrow \Lambda \pi^-$, and $\Lambda \rightarrow p \pi^-$. These studies use a data sample corresponding to an integrated luminosity of 4.2 fb^{-1} and constitute the first exclusive reconstruction of the Ξ_b^0 and the first for the Ξ_b^- in this decay channel.

The CDF II detector has been described in detail elsewhere [8]. This analysis relies upon the tracking system that operates inside a 1.4 T solenoidal magnetic field. A five-layer silicon detector (SVX II) measures track positions at radii of 2.5 to 10.6 cm to provide high precision impact parameter measurements. Each of these layers provides a transverse measurement and a stereo measurement of 90° (three layers) or $\pm 1.2^\circ$ (two layers) with respect to the beam direction. An open-cell drift chamber (COT) covers the radial region from 43 cm to 132 cm and provides track momentum measurement.

Data acquisition is triggered by a system designed to collect particle candidates that decay with lifetimes characteristic of heavy flavor hadrons. The first level of the trigger system requires two tracks in the COT with transverse momentum $p_T > 2.0 \text{ GeV}/c$. In the second level of the trigger, the silicon vertex trigger [9] is used to associate SVX II data with the tracks found in the COT and provides precise impact parameter resolution (typically $40 \mu\text{m}$) for these tracks. The silicon vertex trigger requires two tracks with impact parameters in the range 0.1-1.0 mm with respect to the beam and a point of intersection that is measured with at least a $200 \mu\text{m}$ displacement transverse to the beam.

This analysis combines the trajectories of charged particles to infer the presence of several different hadrons in the decay chains. The decay point for each weak decay process is reconstructed and used to identify the corresponding hadron. Consequently, it is useful to define two quantities in the transverse view that are used to relate the paths of weakly decaying objects to their points of origin. Both quantities make use of the point of closest approach \vec{r}_c of the particle trajectory to a point of origin \vec{r}_o and of the measured particle decay position \vec{r}_d . The first quantity used here is transverse flight distance $f(h)$ of hadron h . For neutral particles, $f(h) \equiv (\vec{r}_d - \vec{r}_o) \cdot \vec{p}_T(h) / |\vec{p}_T(h)|$, where $\vec{p}_T(h)$ is the transverse momentum of the hadron candidate. For charged particles, the flight distance is calculated as the

arc length in the transverse view from \vec{r}_c to \vec{r}_d . Flight distance is used to calculate the proper decay time of weakly decaying states, where the decay time is given by $t \equiv f(h)M(h)/(c|\vec{p}_T(h)|)$, where $M(h)$ is the reconstructed mass. A complementary quantity used in this analysis is transverse impact distance $d(h)$ which is given by $d(h) \equiv |\vec{r}_c - \vec{r}_o|$.

The reconstruction of Λ candidates uses all tracks with $p_T > 0.4 \text{ GeV}/c$ found in the COT. Pairs of oppositely charged tracks are combined to identify these neutral decay candidates, and silicon detector information is not used due to the large transverse displacement of the Λ decay. Candidate selection is based upon the mass calculated for each track pair, which has a resolution of 1.5-2.0 MeV/c^2 and is required to fall within 9 MeV/c^2 of the nominal Λ mass [1] after the appropriate mass assignment for each track. The proton (pion) mass is assigned to the track with the higher (lower) momentum. This mass assignment is always correct for the Λ candidates used in this analysis because of the kinematics of Λ decay and the lower limit in the transverse momentum acceptance of the tracking system. Background to the Λ ($c\tau = 7.9 \text{ cm}$) [1] is reduced by requiring the transverse flight distance of the Λ from the beam position to be greater than 1.0 cm, which corresponds to typically $0.6 \sigma_f$, where σ_f is the flight distance resolution.

For events that contain a Λ candidate, the remaining tracks reconstructed in the COT, again without additional silicon information, are assigned the pion mass, and $\Lambda \pi^-$ combinations are identified that are consistent with the decay process $\Xi^- \rightarrow \Lambda \pi^-$. Several features of the track topology are used to reduce the background to this process. In order to obtain the best possible mass resolution for Ξ^- candidates, the reconstruction requires a convergent fit of the three tracks that simultaneously constrains the Λ decay products to the Λ mass and the Λ trajectory to intersect with the helix of the π^- originating from the Ξ^- candidate. The $\Lambda \pi^-$ mass obtained from this fit has a resolution comparable to the Λ and is required to fall within 9 MeV/c^2 of the nominal Ξ^- mass [1]. In addition, the flight distance of the Λ candidate with respect to the reconstructed decay point of the Ξ^- candidate is required to exceed 1.0 cm. Similarly, due to the long lifetime of the weakly decaying Ξ^- ($c\tau = 4.9 \text{ cm}$) [1], a transverse flight distance of at least 1.0 cm (which typically corresponds to $1.0 \sigma_f$) with respect to the beam position is required.

In some instances, the intersection of the π^- helix with the Λ trajectory produces a situation where two $\Lambda \pi^-$ vertices satisfy the constrained fit and displacement requirements. In addition, the complexity of the Ξ^- and Λ decays allows for occasional combinations where the proper identity of the three tracks is ambiguous. A single, preferred candidate is chosen by retaining only the fit combination with the highest probability of satisfying the constrained fit.

The kinematics of hyperon decay and the lower p_T limit of 0.4 GeV/ c on the decay daughter tracks force the majority of Ξ^- candidates to have $p_T > 1.5$ GeV/ c . This fact, along with the long lifetime of the Ξ^- , results in a significant fraction of the hyperon candidates having decay points located several centimeters radially outward from the beam position. Therefore, we are able to refine the Ξ^- reconstruction by making use of the improved determination of the trajectory that can be obtained by tracking the Ξ^- in the silicon detector. The Ξ^- candidates have an additional fit performed with the three tracks that simultaneously constrains both the Λ and Ξ^- masses of the appropriate track combinations and provides the best possible estimate of the hyperon momentum and decay position. The result of this fit is used to define a helix that serves as the seed for an algorithm that associates silicon detector hits with the Ξ^- track. Candidates with track measurements in at least one layer of the silicon detector have excellent impact distance resolution (typically 60 μm).

The samples of Ξ_c^0 and Ξ_c^+ candidates used in this analysis are obtained by combining the Ξ^- candidates that have SVX II information with additional π^+ candidates. The π^+ candidates are tracks that have been reconstructed with data from at least three SVX II layers. The π^+ used for the Ξ_c^0 reconstruction is required to be consistent with the trigger requirements. The Ξ_c^+ candidates are required to have at least one π^+ track consistent with the trigger requirements. All $\Xi^- \pi^+ (\pi^+)$ combinations are required to satisfy a constrained fit for the three vertices in the decay chain that includes mass constraints on the Λ and Ξ^- candidates. The mass distributions of the combinations that also satisfy $ct > 100 \mu\text{m}$ and $p_T > 4.0$ GeV/ c requirements are shown in Fig. 1. Candidates with a reconstructed mass within 30(25) MeV/ c^2 of the nominal $\Xi_c^0(\Xi_c^+)$ mass are used for b baryon reconstruction.

The $\Xi_b^{(-,0)}$ candidates are reconstructed by combining the $\Xi_c^{(0,+)}$ candidates with π^- candidates that satisfy the trigger requirements. The Ξ_b candidates are required to have $p_T > 6.0$ GeV/ c , restricting the sample to candidates that are within the kinematic range where our acceptance is well modeled [7]. All $\Xi_c \pi^-$ combinations are required to satisfy a constrained fit for the four vertices in the decay chain that includes mass constraints on the Λ , Ξ^- , and Ξ_c candidates. Combinations that are inconsistent with having originated from the collision are rejected by imposing an upper limit on the impact distance d_{PV} of the Ξ_b candidate measured with respect to the primary vertex. In addition, the full reconstruction of the Ξ_b decay chain provides an opportunity to impose a requirement on the decay time of the Ξ_c candidate since both its point of creation and decay are reconstructed.

The mean life of the charm baryons varies over a wide range and is large compared to the typical decay time

resolution of 20 - 60 $\mu\text{m}/c$ that we measure. Therefore, we have chosen a selection on the Ξ_c decay time that uses the decay time resolution σ_t calculated for each candidate and the mean life of the decaying state. The selection is developed by using Λ_b^0 as a reference signal. A sample of $\Lambda_b^0 \rightarrow \Lambda_c^+ \pi^-$ candidates [10] is used to optimize selection criteria for Λ_c^+ decay time based on the mean life of the Λ_c^+ and its decay time resolution. As a result of this study, we require that the measured decay time of the Ξ_c candidate falls within the range $-2\sigma_t < t < 3\tau + 2\sigma_t$ where τ is the mean life of the $\Xi_c^0(c\tau = 33 \mu\text{m})$ and $\Xi_c^+(c\tau = 132 \mu\text{m})$ candidates. This requirement is found to be approximately 95% efficient on our Λ_b^0 ($c\tau = 60 \mu\text{m}$) sample and to reduce the background substantially.

The $\Xi_c^0 \pi^-$ and $\Xi_c^+ \pi^-$ mass distributions with $d_{PV} < 100 \mu\text{m}$ and $ct > 100 \mu\text{m}$ are shown in Fig. 2. These distributions show clear evidence of an excess near a mass of 5.8 GeV/ c^2 with a width consistent with our expected mass measurement resolution. The mass, yield, and significance of the $\Xi_b^{(-,0)}$ signals are obtained by performing an unbinned likelihood fit on the mass distribution of candidates. The likelihood function that is maximized has the form $\mathcal{L} = \prod_i^N (f_s G(m_i, m_0, s_m \sigma_i^m) + (1 - f_s)(a_0 + a_1 m_i))$, where N is the number of candidates in the sample, $G(m_i, m_0, s_m \sigma_i^m)$ is a Gaussian distribution with average m_0 and characteristic width $s_m \sigma_i^m$ to describe the signal, m_i is the mass obtained for a single $\Xi_c^{(0,+)} \pi^-$ candidate, σ_i^m is the calculated uncertainty on m_i , and the a_n terms model the background. The quantities obtained from the fitting procedure include the fraction f_s of the candidates identified as signal, the best average mass value m_0 , a scale factor on the mass resolution s_m to allow for inaccuracy of the resolution estimate, and the values of a_0 and a_1 .

For this data sample, several variations of the fit were used to test the significance. The first of these fits corresponds to the null signal hypothesis, and fixes $f_s = 0.0$, $s_m = 1.0$, and m_0 to the nominal mass of the Ξ_b^- . Additional applications allow f_s to float, retain the constraints on s_m , and fix m_0 to values within 5 MeV/ c^2 of the nominal mass of the Ξ_b^- . The value of $-2 \ln \mathcal{L}$ for the null hypothesis exceeds the values for the fits with variable f_s by at least 48.2 units for the Ξ_b^- candidate sample and by 48.3 units for the Ξ_b^0 candidate sample. We interpret these as equivalent to a χ^2 with one degree of freedom whose probability of occurrence is 3.9×10^{-12} and 3.6×10^{-12} , corresponding to a significance that exceeds 6.8σ for both the Ξ_b^- and Ξ_b^0 . We therefore interpret these results as observations of the processes $\Xi_b^- \rightarrow \Xi_c^0 \pi^-$ and $\Xi_b^0 \rightarrow \Xi_c^+ \pi^-$.

Masses are obtained from the unbinned likelihood fit with the mass and resolution parameters allowed to vary. In addition, the mass fit was used on the $\Xi^- \pi^+$ and $\Xi^- \pi^+ \pi^+$ to obtain mass measurements for the Ξ_c^0 and

Ξ_c^+ , which are seen to be consistent with the nominal values [1]. The results of these fits are listed in Table I.

The accuracy of our mass measurement scale is established by our measurements of the J/ψ , $\psi(2S)$, and Υ masses. These calibration points imply an accuracy of $0.5 \text{ MeV}/c^2$ on the mass measurements of the Ξ_b^- and Ξ_b^0 . Our fitting technique finds that our estimate of the mass resolution on each candidate is low, as listed in Table I. Fits where this scale factor was fixed at 1.0 or 1.4 introduced shifts in our Ξ_b^0 mass result by as much as $1.0 \text{ MeV}/c^2$. A fit with a fixed $20 \text{ MeV}/c^2$ Gaussian width, as implied by the simulation, introduced a shift of only $0.2 \text{ MeV}/c^2$. These effects are added in quadrature with the larger of the asymmetric nominal $\Xi_c^{(0,+)}$ mass uncertainties [1] to yield systematic uncertainties of $1.4 \text{ MeV}/c^2$ for the Ξ_b^- and $1.3 \text{ MeV}/c^2$ for the Ξ_b^0 mass measurements.

The momentum scale uncertainty is common to all of our mass measurements, and can be dropped as a systematic uncertainty of a measurement of the mass difference between the Ξ_b^- and Ξ_b^0 . Our best Ξ_b^- mass measurement of $5790.9 \pm 2.6(\text{stat}) \pm 0.8(\text{syst}) \text{ MeV}/c^2$ [7] is obtained from the $J/\psi \Xi^-$ final state and has a systematic uncertainty that would be reduced to $0.6 \text{ MeV}/c^2$ without this effect. Therefore, we measure the mass difference $M(\Xi_b^-) - M(\Xi_b^0) = 3.1 \pm 5.6(\text{stat}) \pm 1.3(\text{syst}) \text{ MeV}/c^2$, where the statistical and systematic uncertainties of the individual measurements have been added in quadrature.

In conclusion, we have analyzed data collected with the CDF II detector at the Tevatron to observe the bottom, strange baryon Ξ_b^0 . The reconstruction technique is used on the Ξ_b^- as well, and the observation of this state provides a cross check for the analysis. A signal of $25.3_{-5.4}^{+5.6} \Xi_b^0$ candidates, with a significance greater than 6σ , is seen in the decay channel $\Xi_b^0 \rightarrow \Xi_c^+ \pi^-$ where $\Xi_c^+ \rightarrow \Xi^- \pi^+ \pi^+$, $\Xi^- \rightarrow \Lambda \pi^-$, and $\Lambda \rightarrow p \pi^-$. The mass of this baryon is measured to be $5787.8 \pm 5.0(\text{stat}) \pm 1.3(\text{syst}) \text{ MeV}/c^2$, which is consistent with theoretical expectations [2]. In addition, we observe $25.8_{-5.2}^{+5.5} \Xi_b^0$ candidates in the process $\Xi_b^- \rightarrow \Xi_c^0 \pi^-$ where $\Xi_c^0 \rightarrow \Xi^- \pi^+$. The mass measured for the Ξ_b^- is $5796.7 \pm 5.1(\text{stat}) \pm 1.4(\text{syst}) \text{ MeV}/c^2$, which is consistent with our earlier result [7] but does not improve upon it. Neither of these decay channels has been reported previously, and the reconstruction of the Ξ_b^0 is the first observation of this baryon in any channel.

We thank the Fermilab staff and the technical staffs

of the participating institutions for their vital contributions. This work was supported by the U.S. Department of Energy and National Science Foundation; the Italian Istituto Nazionale di Fisica Nucleare; the Ministry of Education, Culture, Sports, Science and Technology of Japan; the Natural Sciences and Engineering Research Council of Canada; the National Science Council of the Republic of China; the Swiss National Science Foundation; the A.P. Sloan Foundation; the Bundesministerium für Bildung und Forschung, Germany; the Korean World Class University Program, the National Research Foundation of Korea; the Science and Technology Facilities Council and the Royal Society, UK; the Institut National de Physique Nucleaire et Physique des Particules/CNRS; the Russian Foundation for Basic Research; the Ministerio de Ciencia e Innovación, and Programa Consolider-Ingenio 2010, Spain; the Slovak R&D Agency; the Academy of Finland; and the Australian Research Council (ARC).

-
- [1] K. Nakamura *et al.* (Particle Data Group), *J. Phys. G* **37**, 075021 (2010).
 - [2] E. Jenkins, *Phys. Rev D* **77**, 034012 (2008); R. Lewis and R. M. Woloshyn, *ibid.* **79**, 014502 (2009); D. Ebert, R. N. Faustov and V. O. Galkin, *ibid.* **72**, 034026 (2005); M. Karliner, B. Keren-Zur, H. J. Lipkin, and J. L. Rosner, *Ann. Phys. (N.Y.)* **324**, 2 (2009); A. Valcarce, H. Garcilazo, and J. Vijande, *Eur. Phys. J. A* **37**, 217 (2008).
 - [3] V.M. Abazov *et al.* (D0 Collaboration), *Phys. Rev. Lett.* **99**, 052001 (2007).
 - [4] T. Aaltonen *et al.* (CDF Collaboration), *Phys. Rev. Lett.* **99**, 052002 (2007).
 - [5] T. Aaltonen *et al.* (CDF Collaboration), *Phys. Rev. Lett.* **99**, 202001 (2007).
 - [6] V. M. Abazov *et al.* (D0 Collaboration), *Phys. Rev. Lett.* **101**, 232002 (2008).
 - [7] T. Aaltonen, *et al.* (CDF Collaboration) *Phys. Rev D* **80**, 072003 (2009).
 - [8] D. Acosta *et al.* (CDF Collaboration), *Phys. Rev. D* **71**, 032001 (2005); A. Sill *et al.*, *Nucl. Instrum. Methods, Sec. A* **447**, 1 (2000); F. Abe *et al.* (CDF Collaboration), *Phys. Rev. D* **50**, 2966 (1994).
 - [9] L. Ristori and G. Punzi, *Ann. Rev. Nucl. Sci.* **60**, 595 (2010).
 - [10] T. Aaltonen, *et al.* (CDF Collaboration) *Phys. Rev. Lett.* **104**, 102002 (2010).

TABLE I: Fit results obtained for c and b baryons.

	Yield	Mass (MeV/c^2)	Resolution Scale
Ξ_c^0	2110 ± 70	2470.4 ± 0.3	1.16 ± 0.04
Ξ_c^+	3048 ± 67	2467.3 ± 0.2	1.24 ± 0.03
Ξ_b^-	$25.8_{-5.2}^{+5.5}$	5796.7 ± 5.1	1.3 ± 0.2
Ξ_b^0	$25.3_{-5.4}^{+5.6}$	5787.8 ± 5.0	1.2 ± 0.2

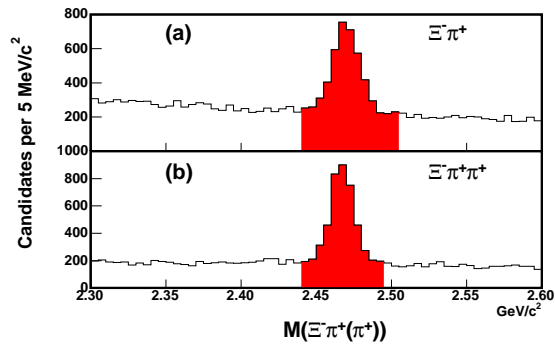


FIG. 1: (a) The $\Xi^-\pi^+$ and (b) the $\Xi^-\pi^+\pi^+$ mass distributions. The mass ranges used for the Ξ_c^0 and Ξ_c^+ samples are indicated by the shaded areas.

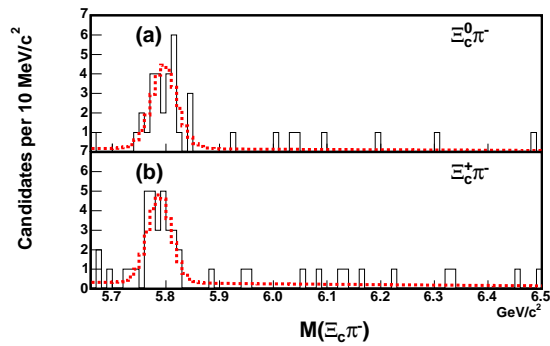


FIG. 2: (a) The $\Xi_c^0\pi^-$ and (b) the $\Xi_c^+\pi^-$ mass distributions. A projection of the likelihood fit is overlaid as a dashed line.